SPEEDAM 2010
International Symposium on Power Electronics,
Electrical Drives, Automation and Motion

A Three-Phase AC/AC Power Electronic Transformer-based PWM AC Drive with Lossless Commutation of Leakage Energy

Kaushik Basu, Apurva Somani, Krushna K Mohapatra, Member, *IEEE* and Ned Mohan Fellow, *IEEE*
Department of Electrical and Computer Engineering
University of Minnesota
Minneapolis, Minnesota 55455
Email: basux017@umn.edu

***Abstract*—This paper presents a novel three-phase ac/ac power converter topology with a high frequency ac-link for adjustable speed PWM ac drives. Such drives find applications in electric power generation from renewable energy sources like wind. This converter has a single power conversion stage with bidirectional power flow capability. The high frequency transformer provides voltage transformation, isolation, noise decoupling and high power density. This topology minimizes the number of switching transitions of the load with the transformer windings. This reduces the common-mode voltage switching and results in a better output voltage profile. This paper presents a lossless source based commutation of leakage energy. It also results in the soft switching of all the switches in the load side converter. The proposed topology is controlled with a carrier based PWM technique based on the direct modulation of matrix converters. This modulation results in controllable input power factor. The proposed converter has been analyzed and simulated. The simulation results confirm the operation and the advantages of the proposed topology.**

I. Introduction

Synthesis of adjustable speed PWM ac from a balanced three phase ac source with a high frequency ac-link has wide range of applications including wind power generation [1]. A transformer in the system provides required voltage transformation along with galvanic isolation. The reason to operate a transformer at high frequency is to reduce its size. This implies increase in power density and reduction in the cost of copper and iron. Conversion of single phase ac to constant frequency adjustable magnitude ac with a high frequency transformer is described in [2] and [3]. In [4], a switching strategy based on phase modulated converter is proposed in order to get soft switching when the output voltage and current are in the same quadrant. Single and three phase ac/ac converters with power electronic transformer based on flyback or push-pull topologies with multiple power conversion stages and reactive elements are proposed in [5], [6] and [7].

This paper focuses on topologies that provide single stage power conversion with bidirectional power flow capability without using any storage elements. In a conventional multi-power stage approach, a rectifier-inverter system has an isolated dc-dc converter in the dc link. This topology has a bulky and unreliable electrolytic capacitor. Matrix converters are well known as a total silicon solution for direct ac/ac power conversion. In literature [8]–[11], there exist two different matrix converter-based approaches for three-phase ac/ac power conversion with a high frequency ac-link.

The first approach is based on indirect modulation of the matrix converter. The virtual dc-link is chopped to a high frequency ac and fed to the transformer by the input converter [8], [9]. The load side converter converts the high frequency ac to adjustable speed and magnitude three-phase ac. In the second approach, first the input three-phase ac is chopped at a high frequency and fed to a bank of three transformers. This can be achieved either by a full-bridge [10] or by a push-pull [11] type of configuration. In the secondary side, a matrix converter is employed to generate output voltage from the high frequency three-phase ac.

Practically, the windings of a transformer have leakage inductances and the load is of inductive nature. In both of the above-mentioned approaches, each switching transition of the output converter requires commutation of the leakage energy. Commutation requires snubber circuits that contain an unreliable electrolytic dc capacitor. The voltage across this capacitor is maintained at a level comparable to the system voltage. This process is lossy. It also increases the voltage rating of the switches. Commutation with snubber circuits results in distortion and loss of the output voltage. It also causes common-mode voltage switching.

This paper proposes a topology (Fig. 1) that minimizes the number of switching transitions between the secondary winding of the transformer and the output load over a period in which the output voltage is synthesized. A lossless source based commutation method of the leakage energy is presented. This commutation method results in soft-switching (ZCS) of all the switches in the load side converter. A carrier based PWM technique is used to modulate the proposed converter and this results in input power factor correction [12]. The advantages of the proposed converter are:

1) Voltage transformation, isolation and high power density
2) Lossless commutation of leakage energy

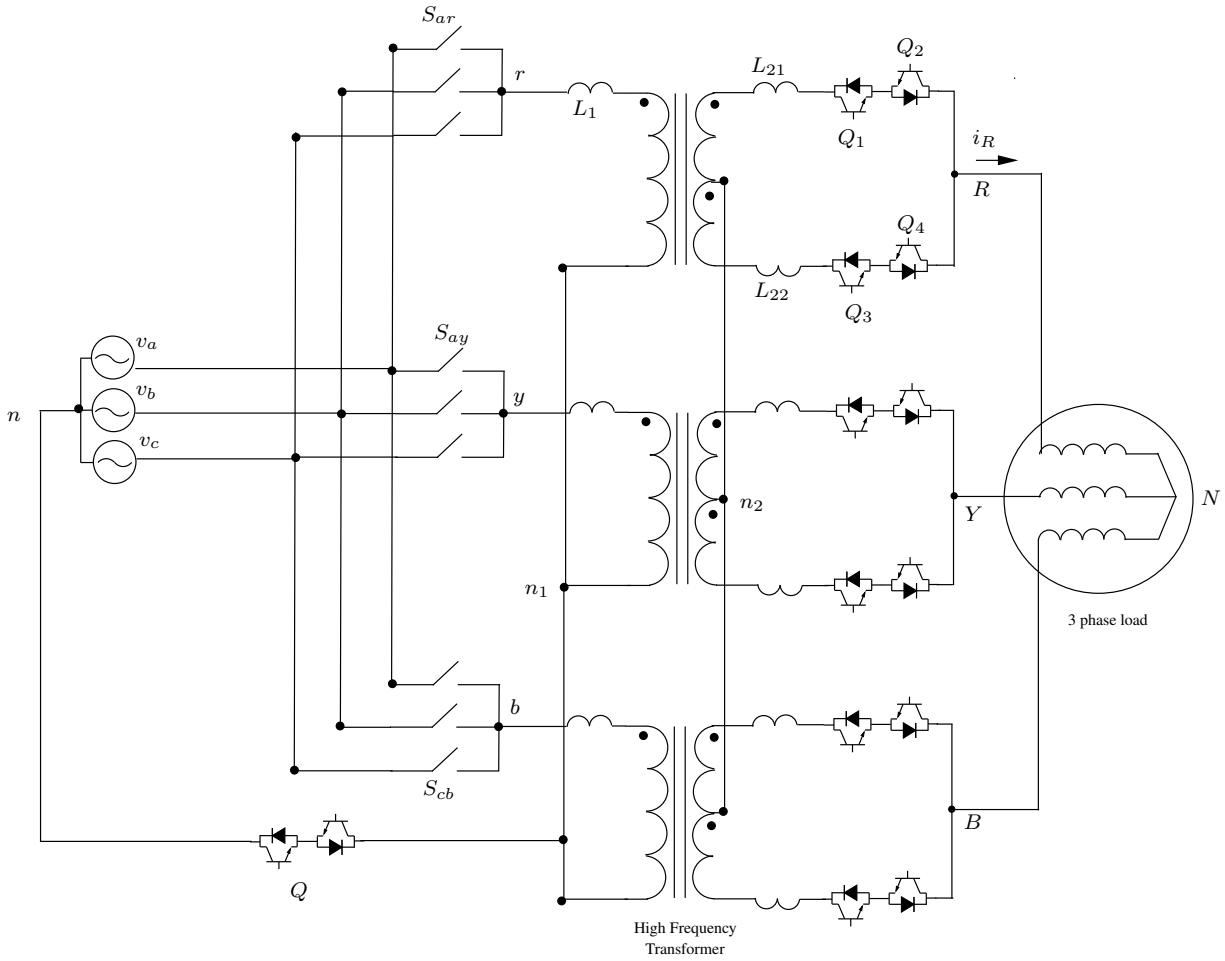

Fig. 1. Circuit diagram of the proposed topology

3) Minimization of the distortion and loss of output voltage
4) No dc-link capacitor
5) Single-stage power conversion with bidirectional power flow capability
6) Input power factor correction
7) Soft-switching

II. Analysis

A. Basic control of the proposed converter

The control of this converter is divided into two parts, output voltage synthesis and commutation. Fig. 2 shows the signals that control these two modes of operation. Modulation of the output voltage happens when PT is high. This stage is further divided into two parts. In the first part Q_1 and Q_2 are ON and power is transferred through the upper half of the secondary windings of each of the three transformers. Similarly during the next part switches Q_3 and Q_4 are ON and the output voltage is synthesized through the lower half of the secondary windings. A switch, Q, is connected between the star point of the primary windings and the neutral of the input three-phase voltage source. During the modulation stage this switch is turned OFF, otherwise a common-mode current will flow.

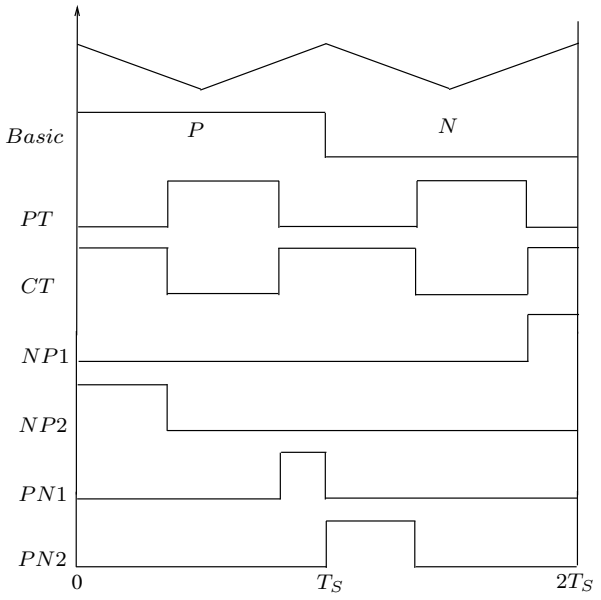

Fig. 2. Control signals

From the primary side, the output three-phase load appears to be in parallel with the star connected magnetizing inductances as shown in Fig.3. In the first half of the mod-

ulation stage, the commanded reference output voltage vector is synthesized on an average by switching the input matrix converter and applied to the transformer primary. In the following half of the modulation stage, negative of the desired output average voltage vector is applied to the transformer primary. The output cycloconverter inverts and applies the desired voltage vector to the load. The average voltage vector applied to the magnetizing inductances over a cycle of operation is zero and this results in the required flux balance in the transformer core.

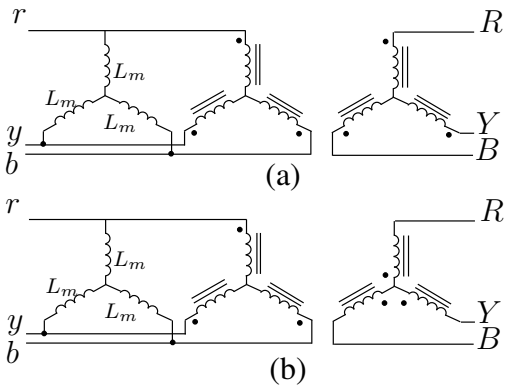

Fig. 3. Circuit configuration during a) positive b) negative states of power transfer

B. Modulation of the input converter

The input converter is modulated with a carrier-based PWM technique [12]. The input three-phase balanced ac voltage source is given by (1). The duty ratio of the switch S_{ar} is denoted by d_{ar}. As the input is connected to a voltage source, no two switches in any leg of the input converter can be ON at the same time. As the output load is inductive in nature, one switch in each leg of the input converter needs to be ON at all times. These requirements result in (2) and (3). The duty ratios of the nine switches of the input converter are given by (4), (5) and (6). Details of the offset duty ratios are given by (7), (8), (9).

$$\begin{aligned} v_a(t) &= V_i \cos \omega_i t \\ v_b(t) &= V_i \cos\left(\omega_i t - \frac{2\pi}{3}\right) \\ v_c(t) &= V_i \cos\left(\omega_i t + \frac{2\pi}{3}\right) \end{aligned} \tag{1}$$

$$\begin{aligned} d_{ar} + d_{br} + d_{cr} &= 1 \\ d_{ay} + d_{by} + d_{cy} &= 1 \\ d_{ab} + d_{bb} + d_{cb} &= 1 \end{aligned} \tag{2}$$

$$\begin{aligned} 0 \le d_{ar}, d_{br}, d_{cr} \le 1 \\ 0 \le d_{ay}, d_{by}, d_{cy} \le 1 \\ 0 \le d_{ab}, d_{bb}, d_{cb} \le 1 \end{aligned} \tag{3}$$

$$\begin{aligned} d_{ar}(t) &= k(t) \cos \omega_o t \cos \omega_i t + D_a + \Delta_a \\ d_{br}(t) &= k(t) \cos \omega_o t \cos\left(\omega_i t - \frac{2\pi}{3}\right) + D_b + \Delta_b \\ d_{cr}(t) &= k(t) \cos \omega_o t \cos\left(\omega_i t + \frac{2\pi}{3}\right) + D_c + \Delta_c \end{aligned} \tag{4}$$

$$\begin{aligned} d_{ay}(t) &= k(t) \cos\left(\omega_o t - \frac{2\pi}{3}\right) \cos \omega_i t + D_a + \Delta_a \\ d_{by}(t) &= k(t) \cos\left(\omega_o t - \frac{2\pi}{3}\right) \cos\left(\omega_i t - \frac{2\pi}{3}\right) \\ &\quad + D_b + \Delta_b \\ d_{cy}(t) &= k(t) \cos\left(\omega_o t - \frac{2\pi}{3}\right) \cos\left(\omega_i t + \frac{2\pi}{3}\right) \\ &\quad + D_c + \Delta_c \end{aligned} \tag{5}$$

$$\begin{aligned} d_{ab}(t) &= k(t) \cos\left(\omega_o t + \frac{2\pi}{3}\right) \cos \omega_i t + D_a + \Delta_a \\ d_{bb}(t) &= k(t) \cos\left(\omega_o t + \frac{2\pi}{3}\right) \cos\left(\omega_i t - \frac{2\pi}{3}\right) \\ &\quad + D_b + \Delta_b \\ d_{cb}(t) &= k(t) \cos\left(\omega_o t + \frac{2\pi}{3}\right) \cos\left(\omega_i t + \frac{2\pi}{3}\right) \\ &\quad + D_c + \Delta_c \end{aligned} \tag{6}$$

$$\begin{aligned} D_a(t) &= 0.5|\cos \omega_i t| \\ D_b(t) &= 0.5\left|\cos\left(\omega_i t - \frac{2\pi}{3}\right)\right| \\ D_c(t) &= 0.5\left|\cos\left(\omega_i t + \frac{2\pi}{3}\right)\right| \end{aligned} \tag{7}$$

$$\Delta_{a,b,c} = \frac{1 - (D_a + D_b + D_c)}{3} \tag{8}$$

$$k(t) = \begin{cases} +k & \text{first half of modulation} \\ -k & \text{next half of modulation} \end{cases} \tag{9}$$

The modulation index is k. The maximum value of modulation index is 0.5. The peak of the line to neutral of the output voltage waveform is kV_{in} where V_{in} is the peak of the input voltage waveform. The angular frequency of the output voltage waveform is ω_o. This modulation leads to input power factor correction [12]. The duty ratio signals are compared with a triangular carrier waveform to generate the gating signals for the switches in the input converter (Fig. 4).

C. Commutation

Commutation refers to the change in the direction of the current in each of the primary windings and transfer of the current from one half of the secondary winding to the other half when the modulation is changing from one state to another. Transformer windings have leakage inductances. In Fig. 1, L_1 refers to the primary

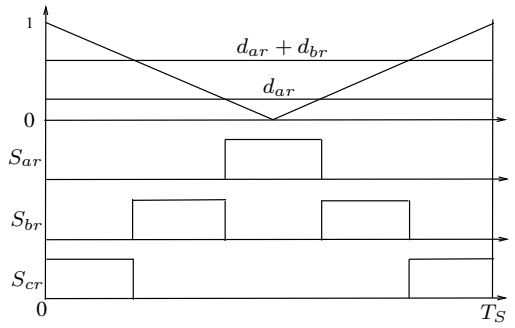

Fig. 4. Front end converter PWM generation

leakage inductance. L_{21} and L_{22} represent the leakage inductances present in the upper and lower half of the secondary winding respectively.

In order to change the current through these leakage inductances a proper voltage needs to be applied. Here the input converter is switched to provide the required voltage from the input ac source. Note that at any instant of time, at least 0.5 times the peak of the input line to neutral voltage is available (in both directions: positive or negative), to be applied across the transformer primary winding of any phase.

Depending on the direction of the output current and the type of change in the modulation state (either upper to lower or otherwise) the commutation process can be classified into four cases. Tables I and II provide the details of the switching schemes for all of these four cases.

As the commutation process is similar for all the three phases, commutation of only one phase (phase-R) is analysed here. Details of one of the four cases of commutation is presented. Figs. 5-9 show the different circuit configurations during commutation when the modulation state is changing from lower to upper state and the load current is negative. Since the commutation period

TABLE I
$i_o > 0$

	Q_1	Q_2	Q_3	Q_4	Q	D_1	D_2	D_3	D_4
P	1	1	0	0	0	0	1	0	0
PN1a	1	0	0	0	1	0	1	0	0
PN1b	1	0	1	0	1	0	1	0	1
N	0	0	1	1	0	0	0	0	1
NP1a	0	0	1	0	1	0	0	0	1
NP1b	1	0	1	0	1	0	1	0	1

TABLE II
$i_o < 0$

	Q_1	Q_2	Q_3	Q_4	Q	D_1	D_2	D_3	D_4
P	1	1	0	0	0	1	0	0	0
PN1a	0	1	0	0	1	1	0	0	0
PN1b	0	1	0	1	1	1	0	1	0
N	0	0	1	1	0	0	0	1	0
NP1a	0	0	0	1	1	0	0	1	0
NP1b	0	1	0	1	1	1	0	1	0

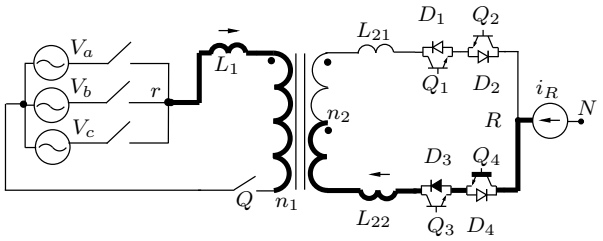

Fig. 5. Circuit configuration: Power transfer through lower half of secondary winding

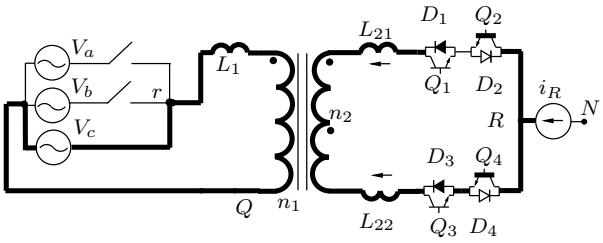

Fig. 6. Circuit configuration: NP1 is high

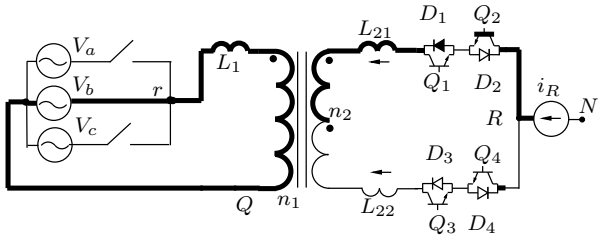

Fig. 7. Circuit configuration: NP2 is high

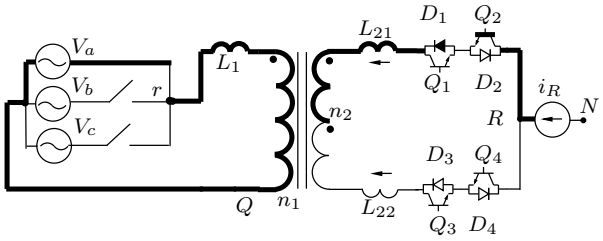

Fig. 8. Circuit configuration: NP2 is high

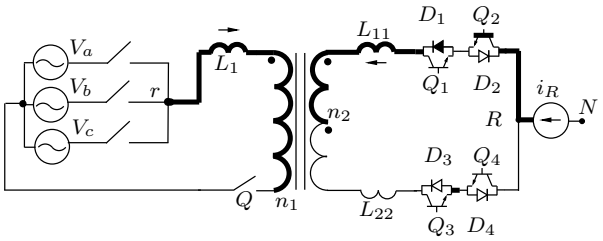

Fig. 9. Circuit configuration: Power transfer through upper half of secondary winding

is much smaller than the time period ($T_o = \frac{2\pi}{\omega_o}$) of the output load current, the load is modeled as a dc current source.

Fig. 5 shows power transfer to the load through the lower half of the secondary winding. Switch Q_4 and diode D_3 are conducting. Switch Q is open during the power transfer mode. The commutation is done on a phase-by-phase basis. A proper voltage needs to be applied to the primary of each phase that is independent of other phases. This is the reason why switch Q is turned ON during commutation. Commutation starts when signal NP1 goes high (Fig 2). The first stage of NP1 is referred to as NP1a in the Tables I and II. At this stage, switch Q_3 is turned OFF and Q is turned ON. This particular commutation requires a negative voltage to be applied to the transformer primary. Say that at this instant of time v_{cn} is most negative input voltage. So the switch S_{cr} is turned ON. During the second stage of NP1 (NP1b), switch Q_2 is turned ON. This forward biases the diode D_1 (Fig. 6) and current i_{21} starts building in the upper half of the primary winding. The equivalent circuit of this stage is given in Fig. 10.

This circuit is analysed in order to find the commutation time. In this analysis the magnetizing component of the transformer current is neglected. Here, N_1 and N_2 are the number of turns in the primary and and each half of the secondary windings. (10) and (11) are obtained using Faraday's and Ampere's law. KCL at load terminal gives equation (12). The next two equations are obtained by applying KVL to the primary and secondary windings. Solution of these equations leads to (15). So the maximum time required to finish the commutation process is given by (16), where, i_{opk} is the maximum value of the peak of the sinusoidal load current. This will ensure sufficient time for commutation at all other load conditions. The moment current i_{21} reaches the load current, i_{22} becomes zero. Because of the diode D_3 the current i_{22} can not become negative and the commutation process ends automatically. The duration of the pulse NP1 must be more than t_{com}. The turn-ON transitions of Q and Q_2 occur with zero current switching (ZCS).

$$\frac{e_1}{N_1} = \frac{e_2}{N_2} \tag{10}$$

$$i_{21}N_2 + i_1N_1 - i_{22}N_2 = 0 \tag{11}$$

$$i_R = i_{21} + i_{22} \tag{12}$$

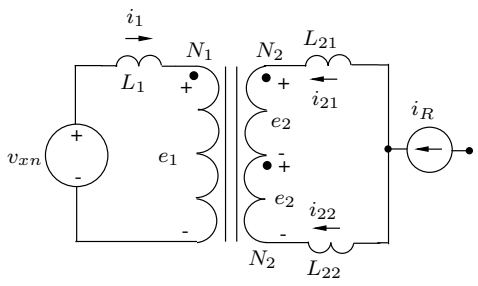

Fig. 10. Equivalent circuit during commutation

$$v_{xn} - e_1 - L_1\frac{d}{dt}i_1 = 0 \tag{13}$$

$$2e_2 + L_{21}\frac{d}{dt}i_{21} - L_{22}\frac{d}{dt}i_{22} = 0 \tag{14}$$

$$\frac{d}{dt}i_{21} = \frac{v_{xn}\left(\frac{N_2}{N_1}\right)}{\left(\frac{L_{21}+L_{22}}{2}\right) + 2L_1\left(\frac{N_2}{N_1}\right)^2} \tag{15}$$

$$\begin{aligned} t_{com} &= \left[\frac{\left(\frac{L_{21}+L_{22}}{2}\right) + 2L_1\left(\frac{N_2}{N_1}\right)^2}{0.5V_{in}\left(\frac{N_2}{N_1}\right)}\right] i_{opk} \\ &= k i_{opk} \end{aligned} \tag{16}$$

When NP2 goes high (Fig. 2), switch Q_4 is turned OFF with ZCS. In order to maintain the true bidirectional nature of the converter switch Q_1 is turned ON. The duration of NP2 is twice of the duration of NP1. The other two input line to neutral voltages are applied to the transformer primary for equal amounts of time during NP2 (Fig. 7 and Fig. 8). The switch current i_Q during the commutation state consists of the sum of the magnetizing currents and the reflected secondary currents of all three phases.

Assume that at this commutation when power transfer is changing from the lower to the upper half of the secondary winding, i_R and i_Y are negative and i_B is positive. Also v_c is the minimum and v_a is the maximum of all input line to neutral voltages. Given the directions of the load currents and the fact they must sum to zero, (17) must be true. The period of time when NP1 is high v_c is applied to r and y phases. v_a is applied to the b phase primary. By (16) we get (18). Here, t_r is the actual time for commutation in phase r. Using (17) and (18) it is possible to show that (19) holds. By solving (10) to (14) we can derive (20). The constant $\bar{k}$ is equal to $\left[1 - \frac{2}{\left(\frac{L_{21}+L_{22}}{2}\right)\left(\frac{N_1}{N_2}\right)^2 + 2L_1}\right]$. The net change in the magnetizing current in phase r during the time period when CT is high is given by (21). L_m is the magnetizing inductance. The time period for which NP1 is high is t_c which is slightly greater than t_{com}. It is $2t_c$ for NP2. In the first half of NP2 (t_c duration) v_b is applied and v_a is used for the remaining time. Similarly it is possible to show $\Delta i_{my} = \frac{t_y}{L_m}\bar{k}v_c$ and $\Delta i_{mb} = \frac{t_b}{L_m}\bar{k}v_a$. The net change in the sum of the magnetizing currents is given in (22). (23) follows from (19) and (22). This implies that the net change in the sum of the magnetizing currents during commutation is zero. Also the sum of the reflected secondary currents (actually the load currents) is zero at this instant of time (when CT is changing its state from high to low)

The switch Q is turned OFF at the end of this period with zero current switching (ZCS). This marks the end of the commutation process. Fig. 9 shows the power transfer through the upper half of the primary winding.

TABLE III
PARAMETERS

L_{load}	$10mH$
R_{load}	2.5Ω
L_1	$15\mu H$
R_1	0.2Ω
L_{21}, L_{22}	$15\mu H$
R_{21}, R_{22}	0.2Ω
L_m	$15mH$

$$|i_R| + |i_Y| = |i_B| \tag{17}$$

$$\begin{aligned} |v_c|t_r &= k|i_R| \\ |v_c|t_y &= k|i_Y| \\ |v_a|t_b &= k|i_B| \end{aligned} \tag{18}$$

$$(t_r + t_y)\, v_c + t_y v_a = 0 \tag{19}$$

$$\begin{aligned} e_r &= \bar{k} v_c \\ e_y &= \bar{k} v_c \\ e_b &= \bar{k} v_a \end{aligned} \tag{20}$$

$$\begin{aligned} \Delta i_{mr} &= \frac{t_r e_r}{L_m} + \frac{(t_c - t_r) v_c}{L_m} + \frac{t_c v_b}{L_m} + \frac{t_c v_a}{L_m} \\ &= \frac{1}{L_m}(t_r e_r - t_r v_c) \\ &= \frac{t_r}{L_m} \bar{k} v_c \end{aligned} \tag{21}$$

$$\sum_{j=r,y,b} \Delta i_{mj} = \frac{\bar{k}}{L_m} \left(t_r v_c + t_y v_c + t_b v_a\right) \tag{22}$$

$$\Delta i_{mr} + \Delta i_{my} + \Delta i_{mb} = 0 \tag{23}$$

D. Simulation results

The circuit in Fig. 1 is simulated in MATLAB/Simulink. V_{in} is set to 500 V. The output is connected to a balanced three phase RL load. The load is star connected. Different parameters of this circuit are given in Table III. The modulation index k is set to 0.25. The frequency ($f_s = \frac{1}{T_s}$) at which the output voltage is generated is 5 kHz. Transformer flux is balanced at 2.5 kHz. The commutation time according to (16) is 6.2 μs. The frequency of the output voltage is 60 Hz.

Fig. 11(b) shows the output load current in phase-R. The peak of this current is slightly less compared to its analytically predicted value. This is due to voltage loss during commutation. Fig. 11(c) gives the current through the upper half of the winding in phase-R. It is clear from this figure that each half of the secondary winding conducts only for 50% of time. Fig. 13 describes the circuit

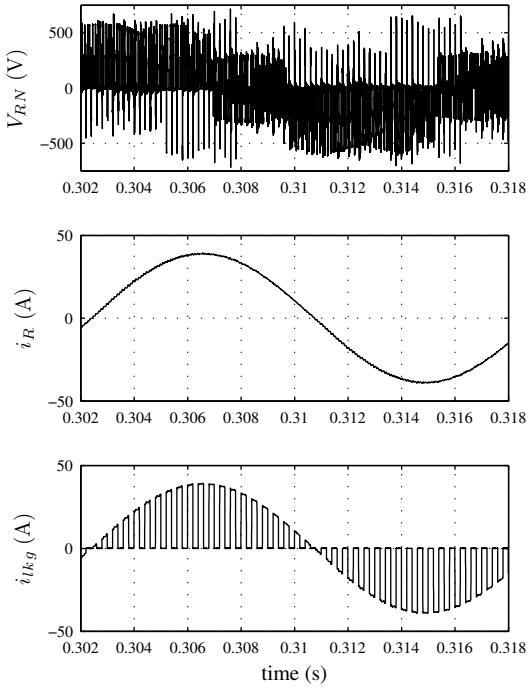

Fig. 11. Simulation result: a) output voltage b) output current c) current through the upper half of secondary winding

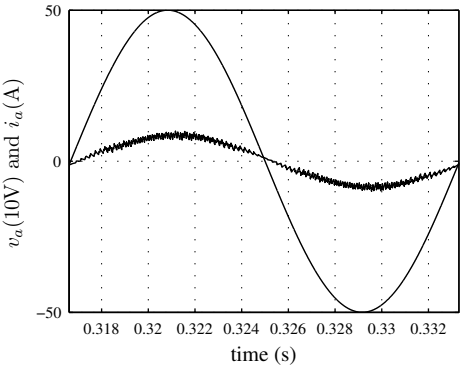

Fig. 12. Simulation results: Input voltage and current(filtered)

operation during commutation. The current through the inductor L_{11} changes linearly during the commutation. Fig. 13(d) shows the current through the switch Q. As the output load is balanced and the net change in the sum of the all three magnetizing currents (Fig. 13(e)) is zero during commutation, the current through switch Q is also zero at the beginning and at the end of the commutation process. These waveforms confirm the soft switching (ZCS) of all of the bidirectional switches. Fig 12 presents filtered input line current waveform with corresponding line to neutral voltage. This confirms input power factor correction. Fig. 14 shows the magnetizing current in one of the phases.

III. CONCLUSION

In this paper, a new power converter topology for direct three-phase ac/ac conversion with a high frequency ac-link has been proposed. This topology offers a single stage

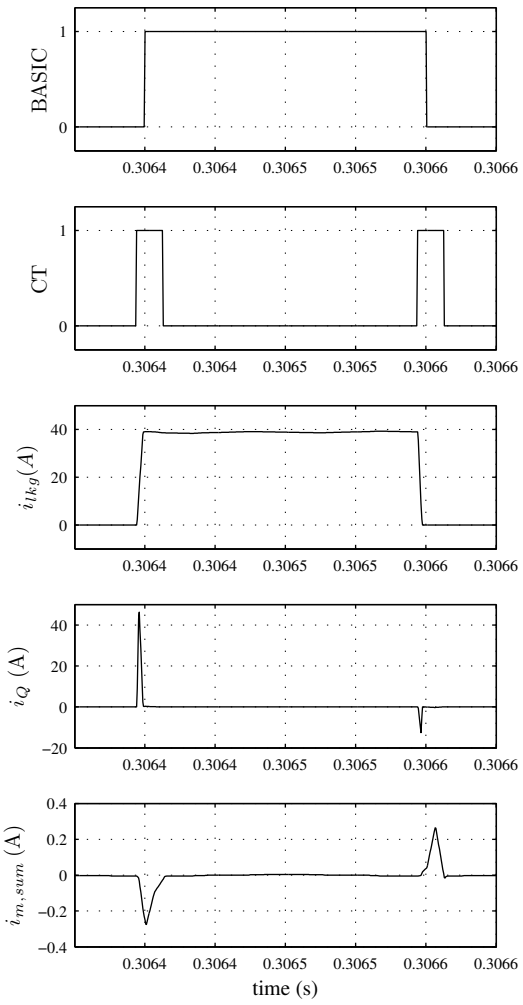

Fig. 13. Simulation results: Commutation process

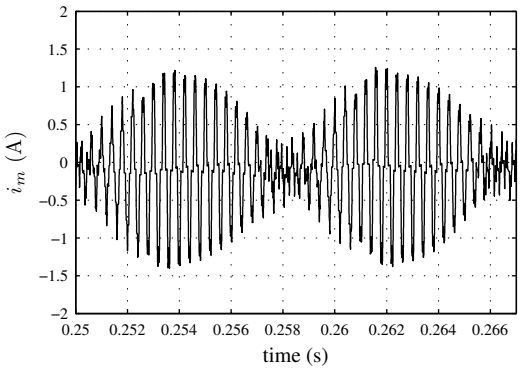

Fig. 14. Simulation results: Magnetizing current

power conversion with bidirectional power flow capability. A control technique has been developed which ensures ZCS in secondary side switches and lossless commutation along with output voltage generation. The circuit has been analysed and its operation for output voltage generation and leakage energy commutation has been described. The following benefits of the proposed topology have been verified through the presented simulation results:

1) Minimum number of switching transitions between the load and the transformer secondary windings. This implies lower distortion and lower loss in the output voltage.
2) Lossless commutation of the leakage energy
3) Zero current switching in all secondary side switches
4) Input power factor correction

This topology is a promising solution for direct ac/ac conversion with high frequency ac-link. However, since the modulation for output voltage generation is done in the input side, the circuit has more number of switches in the input side (usually high voltage) which may be undesirable.

REFERENCES

[1] R. K. Gupta, G. F. Castelino, K. K. Mohapatra, and N. Mohan, "A novel integrated three-phase, switched multi-winding power electronic transformer converter for wind power generation system," in *Proc. Industrial Electronics Society, 2009. IECON'09. The 35th Annual Conference of the IEEE*, Porto, Portugal, Nov. 2009.

[2] M. Kang, P. Enjeti, and I. Pitel, "Analysis and design of electronic transformers for electric power distribution system," in *Industry Applications Conference, 1997. Thirty-Second IAS Annual Meeting, IAS '97., Conference Record of the 1997 IEEE*, vol. 2, Oct 1997, pp. 1689–1694 vol.2.

[3] H. Krishnaswami and V. Ramanarayanan, "Control of high-frequency ac link electronic transformer," *Electric Power Applications, IEE Proceedings* -, vol. 152, no. 3, pp. 509–516, 6 May 2005.

[4] D. Chen and J. Liu, "The uni-polarity phase-shifted controlled voltage mode ac-ac converters with high frequency ac link," *Power Electronics, IEEE Transactions on*, vol. 21, no. 4, pp. 899–905, July 2006.

[5] D. Tang and L. Li, "Analysis and simulation of push-pull three level ac/ac converter with high frequency link," in *Industrial Electronics and Applications, 2009. ICIEA 2009. 4th IEEE Conference on*, May 2009, pp. 3366–3371.

[6] D. Chen, L. Li, J. Liu, S. Lin, and C. Song, "Novel current mode ac/ac converters with high frequency ac link," in *Power Electronics Specialists Conference, 2005. PESC '05. IEEE 36th*, June 2005, pp. 39–44.

[7] M. Manjrekar, R. Kieferndorf, and G. Venkataramanan, "Power electronic transformers for utility applications," in *Industry Applications Conference, 2000. Conference Record of the 2000 IEEE*, vol. 4, Oct 2000, pp. 2496–2502 vol.4.

[8] H. Cha and P. Enjeti, "A three-phase ac/ac high-frequency link matrix converter for vscf applications," in *Power Electronics Specialist Conference, 2003. PESC '03. 2003 IEEE 34th Annual*, vol. 4, June 2003, pp. 1971–1976 vol.4.

[9] K. Basu, A. Umarikar, K. Mohapatra, and N. Mohan, "High-frequency transformer-link three-level inverter drive with common-mode voltage elimination," in *Power Electronics Specialists Conference, 2008. PESC 2008. IEEE*, June 2008, pp. 4413–4418.

[10] K. Mohapatra and N. Mohan, "Matrix converter fed open-ended power electronic transformer for power system application," in *Power and Energy Society General Meeting - Conversion and Delivery of Electrical Energy in the 21st Century, 2008 IEEE*, July 2008, pp. 1–6.

[11] R. K. Gupta, K. K. Mohapatra, and N. Mohan, "A novel three-phase, switched multi-winding power electronic transformer," in *Proc. IEEE Energy Conversion Congress and Exposition (ECCE) 2009*, San Jose, CA, Sep. 2009.

[12] K. Mohapatra, P. Jose, A. Drolia, G. Aggarwal, N. Mohan, and S. Thuta, "A novel carrier-based pwm scheme for matrix converters that is easy to implement," *Power Electronics Specialists Conference, 2005. PESC '05. IEEE 36th*, pp. 2410–2414, 2005.